



Round Mean-field: crowd-opinion-cell

Rome, 27-29 September 2022

Mean-Field limit for hybrid models with chemotaxis: theory and numerics

Marta Menci

Università Campus Bio-Medico di Roma
m.menci@unicampus.it

In collaboration with

Roberto Natalini Istituto per le Applicazioni del Calcolo Consiglio Nazionale delle Ricerche

Thierry Paul CNRS Laboratoire Ypatia des Sciences Mathématiques & Sorbonne Université, Laboratoire Jacques-Louis Lions

Mean-Field limit for hybrid models with chemotaxis: theory and numerics

Outline of the talk

Numerical simulations comparing the different scales

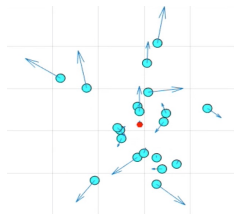
- Basic Hybrid model: discrete particles + chemotaxis
- Mean-field kinetic model: Vlasov equation + chemotaxis
- Hydrodynamic Euler limit: the non monokinetic case

Basic Discrete model with chemotaxis

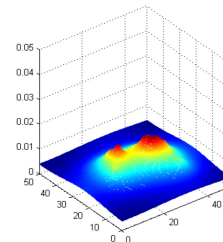
Mechanical interactions

+

Chemotaxis



Evolution in time of each agent's state



Evolution in time of the concentration
of the chemoattractant

Basic Discrete model with chemotaxis

$$\left\{ \begin{array}{l} \dot{x}_i = v_i, \\ \dot{v}_i = \frac{1}{N} \sum_{j=1}^N \gamma(v_i - v_j, x_i - x_j) + \eta \nabla_x \varphi^t(x_i) \\ \partial_t \varphi = D \Delta \varphi - \kappa \varphi + f(x, X(t)) \end{array} \right. \quad \begin{array}{l} \text{Microscopic} \\ \text{Macroscopic} \end{array}$$

The equation block shows a system of three differential equations. The first two equations describe the discrete positions and velocities of N cells. The third equation describes the evolution of the chemoattractant concentration φ over time t . A blue bracket groups the first two equations, with an orange arrow pointing to the word 'Microscopic'. A green arrow points to the word 'Macroscopic' from the third equation.

- x_i Position at time t of the i -th cell
- v_i Velocity at time t of the i -th cell
- φ Concentration of a chemoattractant produced by the cells
- $\gamma(v, x)$ Interaction function among the cells
- $f(x, X)$ Production of chemoattractant

Alignment Models: Cucker Smale (2007)

$$\begin{cases} \dot{x}_i = v_i, \\ \dot{v}_i = \frac{1}{N} \sum_{j=1}^N \gamma(v_i - v_j, x_i - x_j) \end{cases}$$

$$\gamma(v_i - v_j, x_i - x_j) = \frac{1}{(1 + \|x_i - x_j\|^2)^\beta} (v_i - v_j)$$

Cucker-Smale influence function

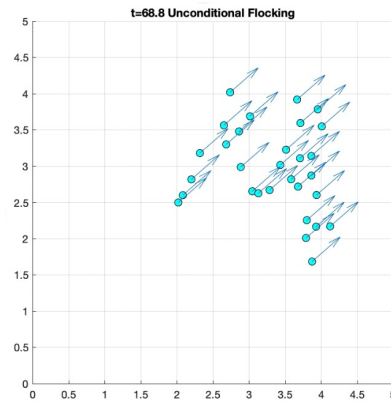
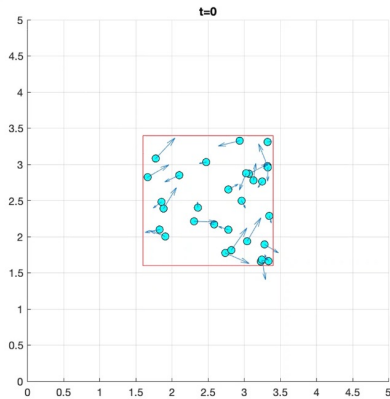
$$\beta \leq \frac{1}{2}$$

Unconditional flocking behavior

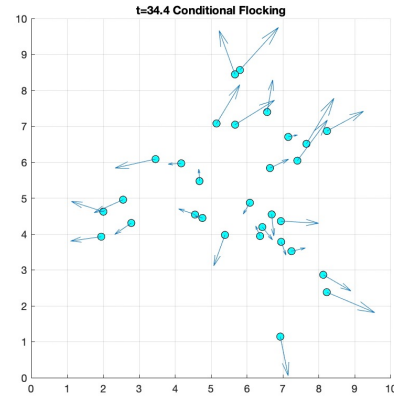
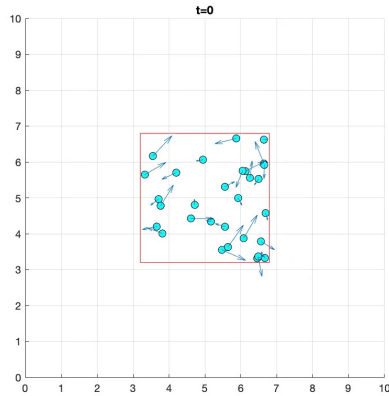
$$\beta > \frac{1}{2}$$

Conditional flocking behavior

Unconditional Flocking



Conditional Flocking



The effect of chemicals

$$\begin{cases} \dot{x}_i = v_i, \\ \dot{v}_i = \frac{1}{N} \sum_{j=1}^N \gamma(v_i - v_j, x_i - x_j) + \eta \nabla_x \varphi^t(x_i) \\ \partial_t \varphi = D \Delta \varphi - \kappa \varphi + f(x, X(t)) \end{cases}$$



$$\gamma(v_i - v_j, x_i - x_j) = \frac{1}{(1 + \|x_i - x_j\|^2)^\beta} (v_i - v_j)$$

Cucker-Smale influence function



$$f(x, X(t)) = \sum_{j=1}^N \chi_{\mathbf{B}(\mathbf{x}_j, R)}$$

Cells = regions from which signal arises

sum of characteristic functions
on balls of radius R, centered in each particle

The effect of chemicals

$$\left\{ \begin{array}{l} \dot{x}_i = v_i, \\ \dot{v}_i = \frac{1}{N} \sum_{j=1}^N \gamma(v_i - v_j, x_i - x_j) + \eta \nabla_x \varphi^t(x_i) \\ \partial_t \varphi = D \Delta \varphi - \kappa \varphi + f(x, X(t)) \end{array} \right.$$

Analytical Results

- Global existence and uniqueness of the solution in \mathbb{R}^2
- Asymptotic properties

Asymptotic properties on the linearised system

$$\mathbf{X}_{CM}(t) := \frac{1}{N} \sum_{i=1}^N \mathbf{X}_i(t),$$

$$\mathbf{V}_{CM}(t) := \frac{1}{N} \sum_{i=1}^N \mathbf{V}_i(t),$$

- 1) Velocity and position of all particles converge to the same values (their centre of mass)
- 2) The velocity of the centre of mass decays to zero



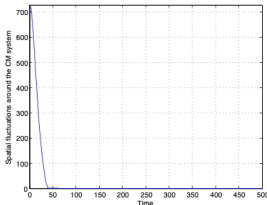
Time-asymptotic flocking condition

Stronger condition: Particles converge to their centre of mass

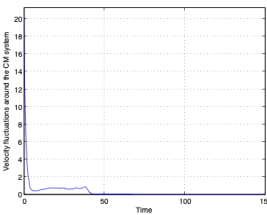
Velocity decays to zero



Agreement between analytical and numerical results on the full system

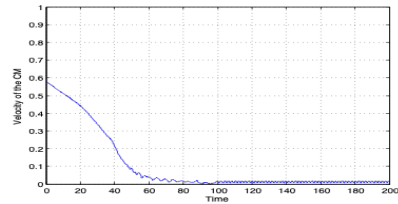


$$\blacktriangleright FI_x(t) := \sum_{i=1}^n \|\mathbf{x}_i(t) - \mathbf{x}_{CM}(t)\|^2 \rightarrow 0$$



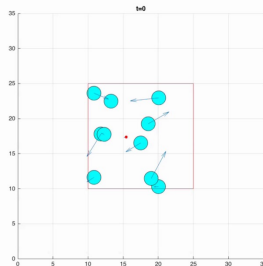
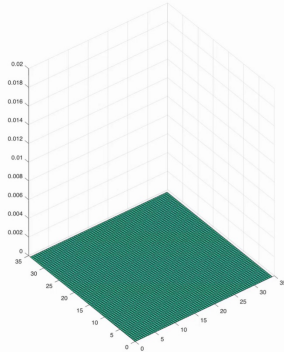
$$\blacktriangleright FI_v(t) := \sum_{i=1}^n \|\mathbf{v}_i(t) - \mathbf{v}_{CM}(t)\|^2 \rightarrow 0$$

$$\blacktriangleright \|\mathbf{v}_{CM}(t)\|^2 \rightarrow 0$$





Chemotaxis plays a crucial role: time-asymptotic flocking behavior is ensured for any value of $\beta > 0$



Di Costanzo E., Menci M., Messina E., Natalini R. and Vecchio A. (2020). *A hybrid model of collective motion of discrete particles under alignment and continuum chemotaxis*. *Discrete Cont. Dyn-B*, 25(1), 443–472. (doi: 10.3934/dcdsb.2019189)

Mean-field kinetic equation

$$\partial_t \rho^t(x, v) + v \cdot \nabla_x \rho^t(x, v) + \nabla_v \cdot \left(\rho^t(x, v) \int_{2d} \psi(x - y)(v - w) \rho^t(y, w) dy dw \right) = 0$$

► Numerical aspects

J.A. Carrillo, M. Fornasier, G. Toscani, and F. Vecil. *Particle, kinetic, and hydrodynamic models of swarming*. Mathematical modeling of collective behavior in socio-economic and life sciences (2010)

G. Albi, and L. Pareschi. *Binary interaction algorithms for the simulation of flocking and swarming dynamics*. Multiscale Modeling & Simulation (2013)

Different binary interaction methods for solving the kinetic equation

Comparison of Cucker-Smale model in absence/ presence of visual limitations (perception cone)

1D Numerical Simulations

$$\partial_t \rho^t(x, v) + v \cdot \nabla_x \rho^t(x, v) + \nabla_v \cdot \left(\rho^t(x, v) \int_{2d} \psi(x - y)(v - w) \rho^t(y, w) dy dw \right) = 0$$

$$\rho^0(x, v) = \frac{1}{2\pi\sigma_x\sigma_v} e^{\frac{-x^2}{2\sigma_x^2}} \left(e^{\frac{-(v + v_0)^2}{2\sigma_v^2}} + e^{\frac{-(v - v_0)^2}{2\sigma_v^2}} \right)$$



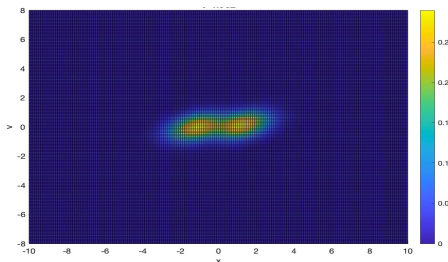
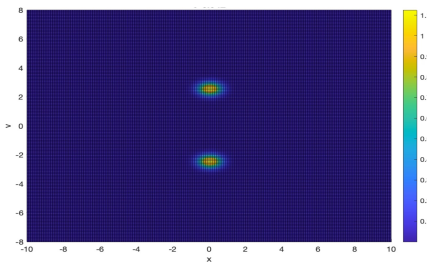
Finite Difference scheme

No perception cone

Simulations for $\beta = 0.05$ and $\beta = 0.95$

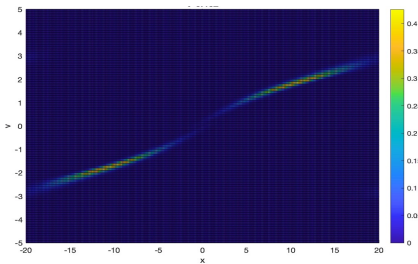
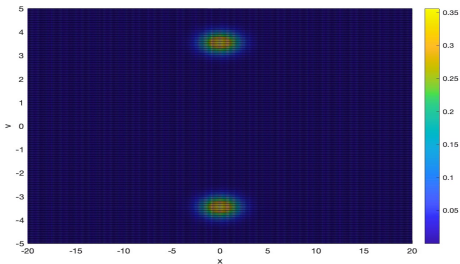
$$\partial_t \rho^t(x, v) + v \cdot \nabla_x \rho^t(x, v) + \nabla_v \cdot \left(\rho^t(x, v) \int_{2d} \psi(x - y)(v - w) \rho^t(y, w) dy dw \right) = 0$$

1D Cucker-Smale flocking in the phase space ($\beta = 0.05$)



$$\partial_t \rho^t(x, v) + v \cdot \nabla_x \rho^t(x, v) + \nabla_v \cdot \left(\rho^t(x, v) \int_{2d} \psi(x - y)(v - w) \rho^t(y, w) dy dw \right) = 0$$

1D Cucker-Smale flocking in the phase space ($\beta = 0.95$)



The effect of chemotaxis



$$\begin{cases} \partial_t \rho^t + v \cdot \nabla_x \rho^t = \nabla_v(\nu(t, x, v) \rho^t), \quad \rho^0 = \rho^{in} \\ \nu(t, x, v) = \gamma(x, v) * \rho^t + \eta \nabla_x \psi^t(x) + F_{ext}(x), \\ \partial_s \psi^s(z) = D \Delta_z \psi - \kappa \psi + g(z, \rho^s), \quad \psi^0 = \varphi^{in} \end{cases}$$

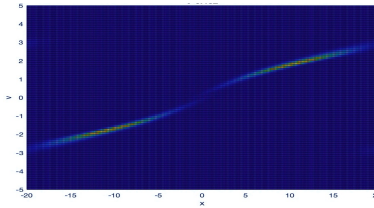
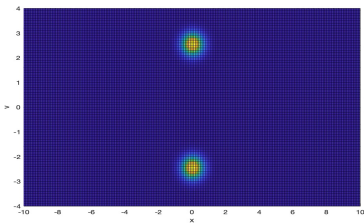


Neglect external forces

Alignment interaction

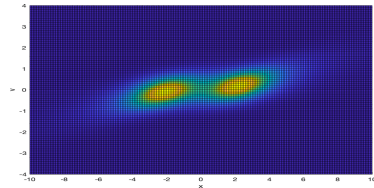


As in the microscopic scale, chemotactic effects leads to consensus



$\eta = 0$

No flocking



$\eta > 0$

Flocking



Non local hybrid Euler system

$$\begin{cases} \partial_t \mu^t + \nabla_x (u^t \mu^t) = 0 \\ \partial_t (\mu^t u^t) + \nabla (\mu^t (u^t)^{\otimes 2}) = \mu^t \int \gamma(\cdot - y, u^t(\cdot) - u^t(y)) \mu^t(y) dy + \mu^t \nabla \psi^t \\ \partial_s \psi^s(z) = D \Delta_z \psi - \kappa \psi + \chi * \mu^s \end{cases}$$



Pressureless Euler-type system

+

Chemotaxis

► Neglecting chemotaxis

$$\begin{cases} \partial_t \mu^t + \nabla_x (u^t \mu^t) = 0 \\ \partial_t (\mu^t u^t) + \nabla (\mu^t (u^t)^{\otimes 2}) = \mu^t \int \gamma(\cdot - y, u^t(\cdot) - u^t(y)) \mu^t(y) dy \end{cases}$$



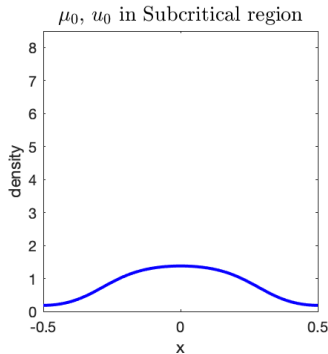
Condition on initial data for global consensus.

Finite-time blow up of the solutions.

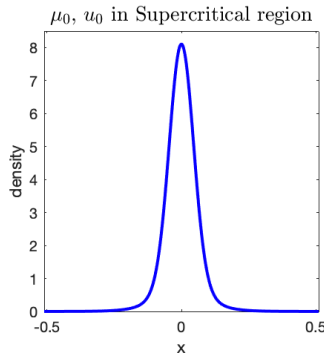


Relaxation Schemes for conservation laws (Aregba-Driollet & Natalini 2000)

Consensus



Finite-time blow up

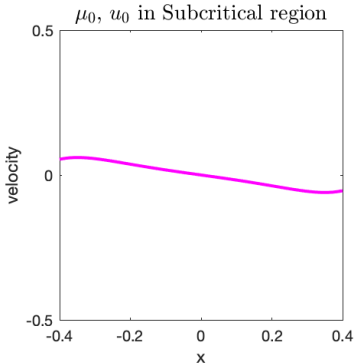


density value at the origin
gets larger and larger...

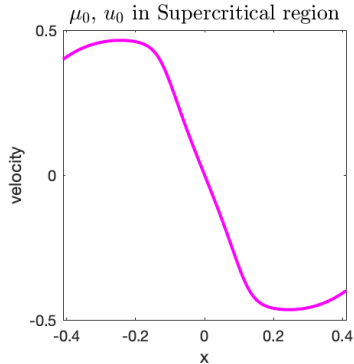


Pressureless Euler-type system

Consensus



Finite-time blow up



the derivative of the velocity becomes sharper and sharper at the origin



The effect of chemotaxis



$$\begin{cases} \partial_t \mu^t + \nabla_x (u^t \mu^t) = 0 \\ \partial_t (\mu^t u^t) + \nabla (\mu^t (u^t)^{\otimes 2}) = \mu^t \int \gamma(\cdot - y, u^t(\cdot) - u^t(y)) \mu^t(y) dy + \mu^t \nabla \psi - \nu \mu^t u^t \\ \partial_s \psi^s(z) = D \Delta_z \psi - \kappa \psi + \chi * \mu^s \end{cases}$$

Does the damping term and/or chemotaxis prevent blow up phenomena?

Damping term	Chemotactic gradient	Finite-time blow up
		✓
	✓	
✓		
✓	✓	

Analytical result: the monokinetic case



Theorem 7.1. Let μ^t, u^t, ψ^t solves the following system

$$\begin{cases} \partial_t \mu^t + \nabla_x (u^t \mu^t) = 0 \\ \partial_t (\mu^t u^t) + \nabla (\mu^t (u^t)^{\otimes 2}) = \mu^t \int \gamma(\cdot - y, u^t(\cdot) - u^t(y)) \mu^t(y) dy + \nabla \psi^t + F \\ \partial_s \psi^s(z) = D \Delta_z \psi - \kappa \psi + \chi * \mu^s, \quad s \in [0, t], \\ (\mu^0, u^0, \psi^0) = (\mu^{in}, u^{in}, \psi^{in}) \in H^s, \quad s > \frac{d}{2} + 1. \end{cases}$$

where $\mu^t, u^t \in C([0, t]; H^s) \cap C^1([0, T]; H^{s-1})$, $\psi^t \in C([0, t]; H^s) \cap C^1([0, T]; H^{s-2}) \cap L^2(0, T; H^{s+1})$ ³.

Then $\rho^t(x, v) := \mu^t(x) \delta(v - u^t(x))$ solves the following system

$$\begin{cases} \partial_t \rho^t + v \cdot \nabla_x \rho^t = \nabla_v (\nu(t, x, v) \rho^t), \\ \nu(t, x, v) = \gamma(x, v) * \rho^t + \eta \nabla_x \psi^t(x) + F_{ext}(x), \\ \partial_s \psi^s(z) = D \Delta_z \psi - \kappa \psi + g(z, \rho^s), \quad \psi^0 = \psi^{in} \\ \rho^0(x, v) = \mu^{in}(x) \delta(v - u^{in}(x)). \end{cases}$$

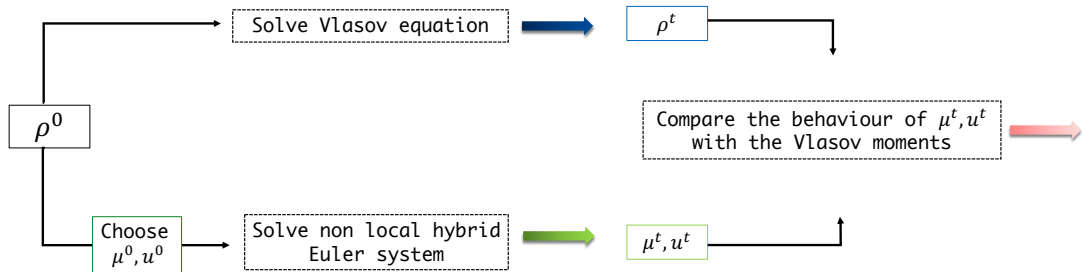
Numerical results: the general case



In the monokinetic case, Vlasov moments and Euler solutions coincide.
What about the non monokinetic case?

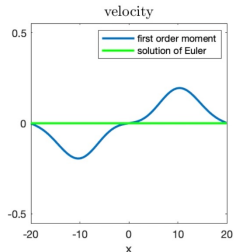
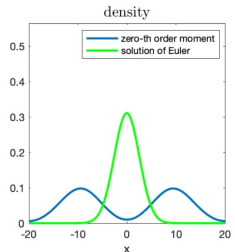
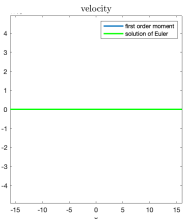
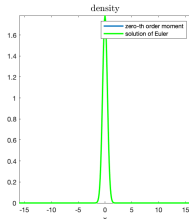


Numerical comparison between moments of Vlasov equation and solutions of the non local hybrid Euler system



Numerical results: the general case

► Neglecting chemotaxis



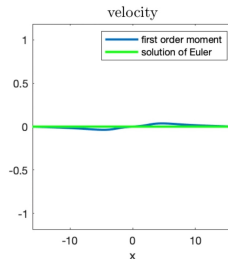
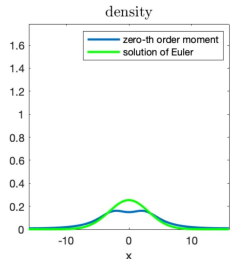
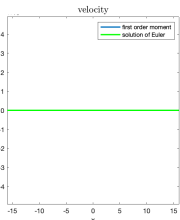
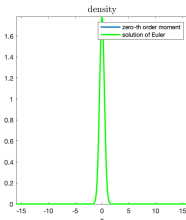
Numerical evidence:

No good agreement in the non monokinetic case



Numerical results: the general case

With chemotaxis



Numerical evidence:

good agreement even in the non monokinetic case



Mean-Field limit for hybrid models with chemotaxis: theory and numerics

Conclusions and beyond

- The different features of the microscopic dynamics are still present in numerical simulations of Vlasov and non local hybrid Euler system
- Numerical investigations on the non monokinetic case
- The role of chemotaxis at different scale
- Different kind of interactions
- Compare the non local hybrid Euler system and Euler models with pressure for chemotaxis



2022

Round Mean-field: crowd-opinion-cell

Rome, 27-29 September 2022

Thanks for your attention

Marta Menci
Università Campus Bio-Medico di Roma
m.menci@unicampus.it

